CHAPTER 8

THE ENERGY SAVER IN TEVATRON I

8.1 Functions of the Energy Saver in Tevatron I

The Tevatron I project uses the Energy Saver Ring as a 1-TeV storage ring for bunched-beam collisions. The construction of this ring was a separate project undertaken for the purpose of operating the Fermilab fixed-target program at 500 GeV. It was recognized that the Energy Saver could be used as a 1-TeV storage ring if proper attention was given to a number of details such as position monitors and beam-transfer systems.[1] Since the field quality for slow extraction was at least as stringent as the requirement for colliding beams, the Energy Saver is inherently a useful storage ring. For that reason, the Energy Saver was designed so that it could be modified in the future to operate as a 1-TeV collider. These modifications are part of the Tevatron I project.

The Energy Saver will perform the following functions in the Tevatron I project:

1. Injection. It will sequentially accept bunches of 150-GeV protons and antiprotons from the Main Ring, one bunch at a time.

2. Acceleration. After the appropriate number of bunches has been stored, it will simultaneously accelerate the proton and antiproton bunches to the collision energy.

3. Collision. After acceleration, the beams will be stored and the low-beta sections described in Chapter 9 will be turned on to increase the luminosity.

The material presented in Sections 8.2 and 8.3 is based on the Superconducting Accelerator Design Report, May, 1979. Since 1979, there have been a number of changes in the design. The changes that are important to the use of the Energy Saver as a collider are described in this chapter. The most notable of these are: the correction coils are separate from the quadrupole windings, the rf system has been expanded to handle the larger longitudinal emittance of the antiprotons, and the beam transfer at E0 has been simplified substantially after it was decided to make the circumference of the Energy Saver exactly the same as the Main Ring.

8.2 Energy Saver Lattice

8.2.1 Ring Location and Normal Lattice. The lattice of the Energy Saver ring is constrained by the requirement that it fit beneath the Main Ring magnets. Therefore, it has the same basic configuration as the Main Ring,

which has 6 superperiods with 6 long straight sections and normal cells with 8 dipoles and 2 quadrupoles. Because the Energy Saver dipole ends could not be placed directly under the Main Ring ends, the Energy Saver dipoles are displaced 15.5 in. upstream of their Main Ring counterparts.[2] Figures 8-1 and 8-2 sketch the position of the quadrupole in the lattice and the position of a normal cell relative to the Main Ring lattice. The beam center line is 25.5 inches below Main Ring center line. The circumference of the two rings is identical. At the time the Superconducting Accelerator Design Report was prepared, it was proposed to make the two rings differ in circumference by 4.4 cm, as a way of providing for pp collisions with the Main Ring and Saver. That option has been dropped because it compromised the beam transfer between the Main Ring and the Saver.[3]

Like the Main Ring, the present lattice has a medium straight section at location 17 formed by omitting two dipoles. Its layout is shown in Fig. 8-3. There are long straight sections of "normal" configuration, ones with high beta for extraction, and ones with low beta for colliding-beam interactions. These are discussed separately in subsequent sections. Table 8-I summarizes the warm straight-section lengths available in the lattice. It gives the drift lengths between "effective" magnetic ends of the elements, the available warm length and the space allotted for the cryogenic bypasses of cold-to-warm transitions and vacuum isolation.

TABLE 8-I WARM STRAIGHT-SECTION LENGTHS

Location of Warm Regions (In.)	Drift Length[a] (In.)	Available Warm Length (In.)	Hot-Cold Transition Upstream	Hot-Cold Transition Downstream
Median location 17 (standard quadrupole with corrections)	566.2	493.2	39	34
Normal-β median location 48	310.9	238.9	36	36
High-β median location 48	308.7	236.7	36	36
Normal-β doublet space 49,11	150.36	78.36	36	36
High-β doublet space 49,11	151.65	79.65	36	36
Long straight section	2094.2	2022.2	36	36
Low-β long straight section	600.24	528.24	36	36

[a]Magnetic lengths used throughout to define drift lengths.

All medium straight sections at 17 and 48 locations, and all long straight sections are warm. The space between the long straight-section doublets is warm only where necessary.

8.2.2 Normal and High-Beta Long Straight Sections. Figure 8-4 shows the geometry of the normal long straight section together with amplitude

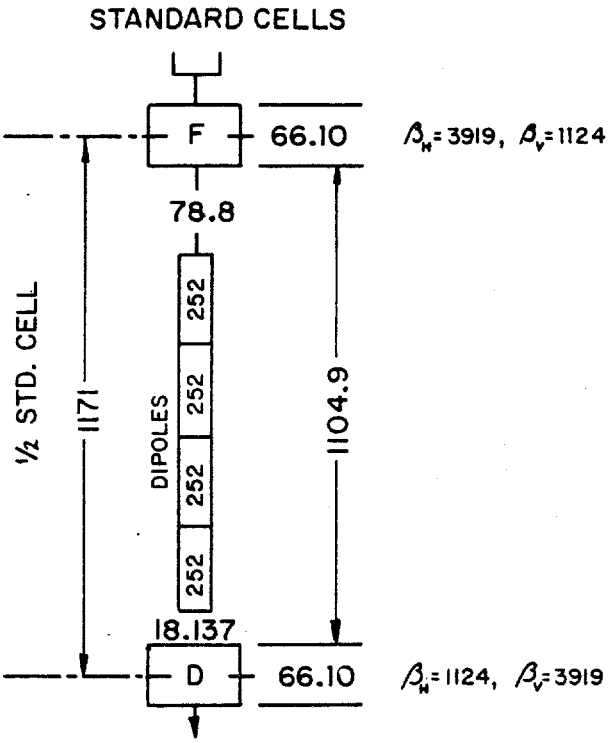

All dimensions in inches, slot length for dipoles, effective magnetic length for quads except for focussing, D-F 1/2-cell is similar.

Phase advance 1/2-cell = 33.903°

Figure 8-1 Locations of elements in standard cell.

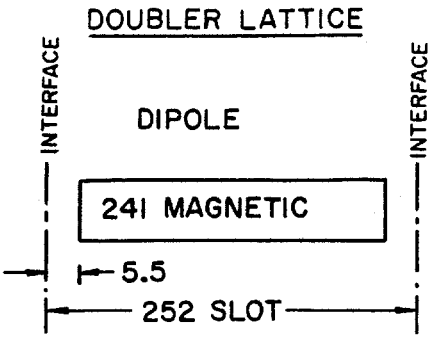

Dipoles are 252" flange to flange. Assume effective magnetic length $\ell = \frac{1}{B_0}\int B d\ell = 241"$. Each Dipole bends $\theta = 2\pi/774$ Rad. Quads are in series with bends. At a current (nom. 4527A) when dipole $B_0\ell$ = 245 kG x 241", I assume a quad grad. G_0 =19.627 kG/in or $k = (G_0\theta/B_0\ell)^{\frac{1}{2}}$ = .003833/in.

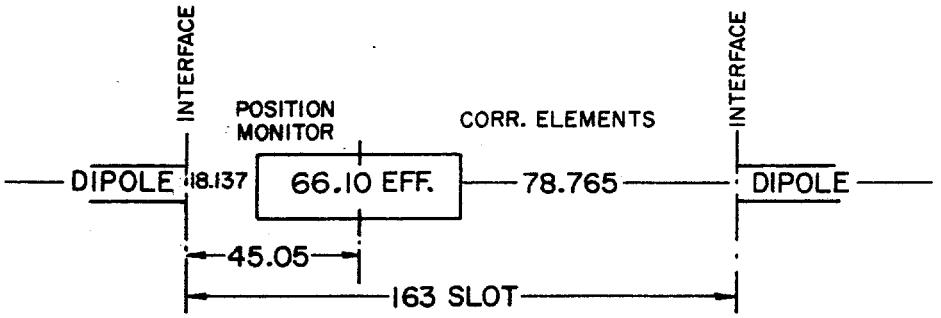

Standard quad. Showing effective length $\frac{1}{G_0}\int G d\ell$ and its position in cryostat. There are many non standard quads.

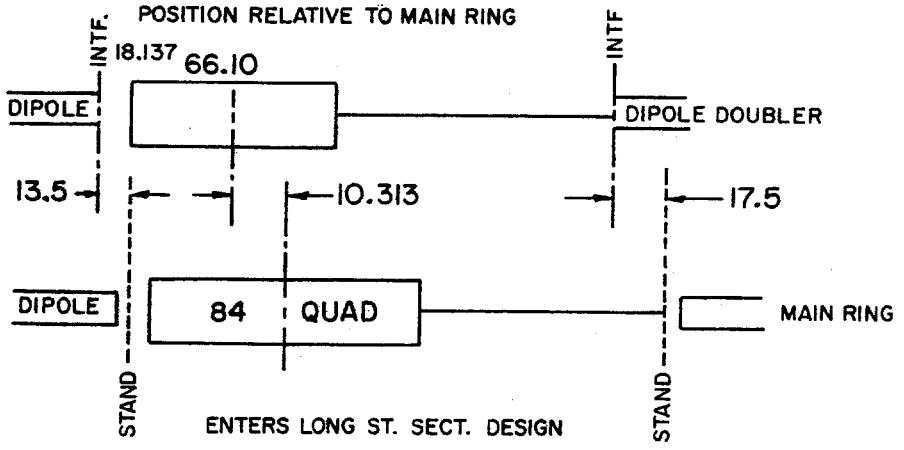

Figure 8-2 Locations of superconducting magnets relative to Main Ring.

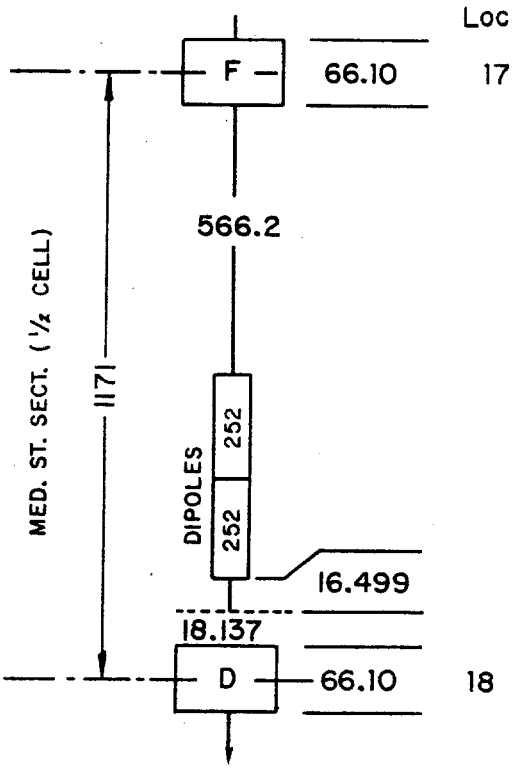

Figure 8-3 Medium straight section. A standard 1/2-cell with two dipoles omitted. A space of 16-1/2 inches must be inserted at downstream end to close the geometric orbit in the shifted Doubler.

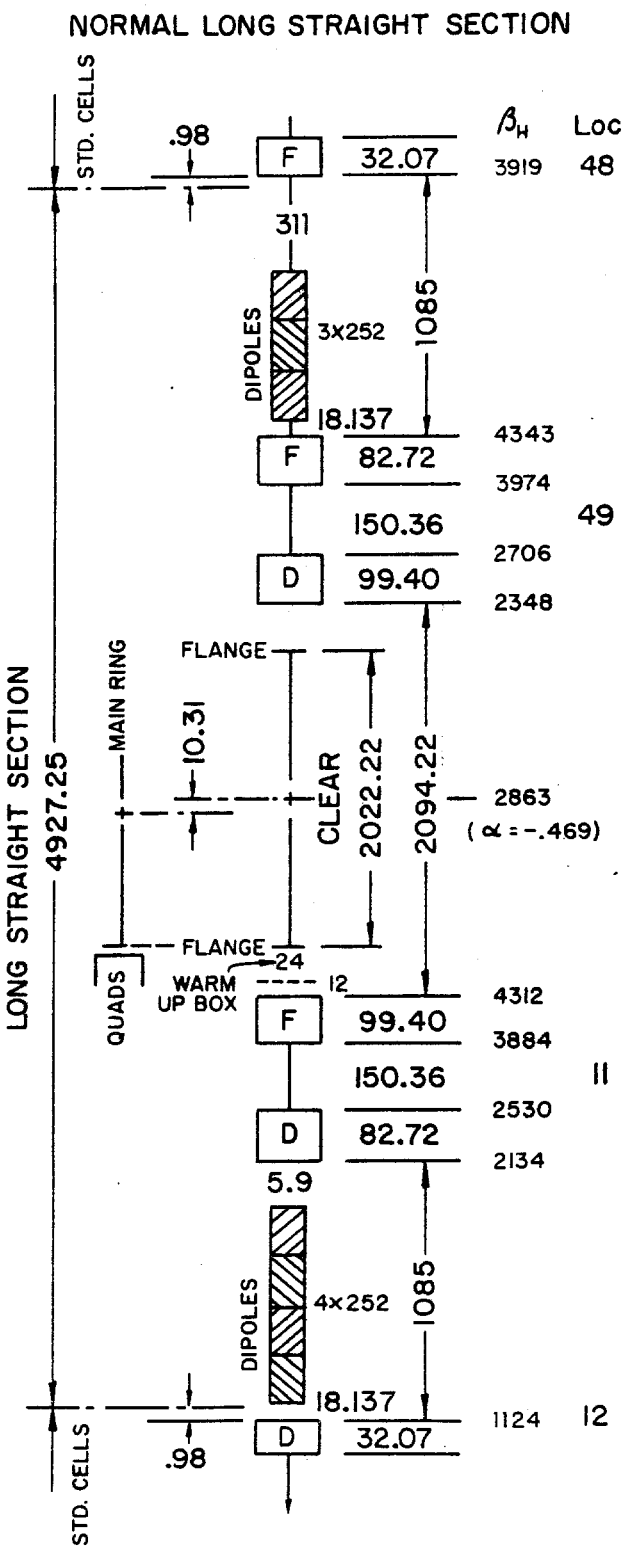

All dimensions in inches

Dipoles in slot length
Quads in eff. gradient length

Note: end quads are shorter than 1/2 standard quad so first "element" of long st. section removes .98" of quad from last standard cell

Main Ring at st. section center has β = 2863, α = -.725
injection matching requires weak F quad at center of transfer line

17.6 kG @ 150 GeV/c

Effective phase advance for long st. section 113.04°
(84.02° for sector)

For β_V read backwards

Figure 8-4 Normal long straight section.

functions. The design is very similar to normal Main Ring straight sections with the exception that two, rather than four, quadrupoles are used at either end of the straight section. CO, EO, FO are normal long straight sections. With this choice for EO, the lattice functions of the Main Ring and Energy Saver are matched nicely for the purpose of beam transfer.

The high-beta long straight section is illustrated in Fig. 8-5. Here the order of focusing in the doublets is reversed and lengths of all six quadrupoles are slightly changed. A large horizontal beta is produced at the upstream end of the straight section. High-beta straight sections were chosen for AO and DO because they facilitated resonant extraction, which places the most severe demands on the size of the good-field aperture. Since the good-field aperture of the superconducting magnets is not large, the use of high-beta at this location of the extraction electrostatic and magnetic septa reduces the aperture required for extraction in the rest of the magnet ring. This choice, which was made for fixed-target operation, will not affect the collider performance.

8.2.3 Lattice Elements. Table 8-II lists the various elements required for a ring incorporating two high-beta long straight sections and four normal long straight sections. The lengths shown are magnetic lengths in inches.

TABLE 8-II LATTICE ELEMENTS

Element	Magnetic Length (In.)	Number
Dipole	241.0	774
Standard quadrupole	66.1	180
Long straight inner quadrupole	99.4	12
Normal long straight short quadrupole (48,12 location)	32.07	8
Outer quadrupole	82.72	8
High beta long straight short quadrupole (48,12 location)	25.5	4
Outer quadrupole	90.19	4

8.2.4 Low-Beta Long Straight Section. The low-beta straight section at BO is made by replacing the 32.07 in. quadrupoles at each end of the normal straight section with stronger, separately powered 66.10 in. quadrupoles and adding eight additional quadrupoles within the 2054 in.clear space around BO. During injection these eight quadrupoles are turned off and the two 66.10 in. quadrupoles are excited to a lower current than those in the rest of the ring. After injection and acceleration, the inner eight quadrupoles are turned on, and all ten quadrupoles are slowly adjusted until the final beta-value of 1 m is reached. This process is described in detail in Chapter 9. It is noted that these eight quadrupoles will be turned off during fixed-target operation. The additional elements required

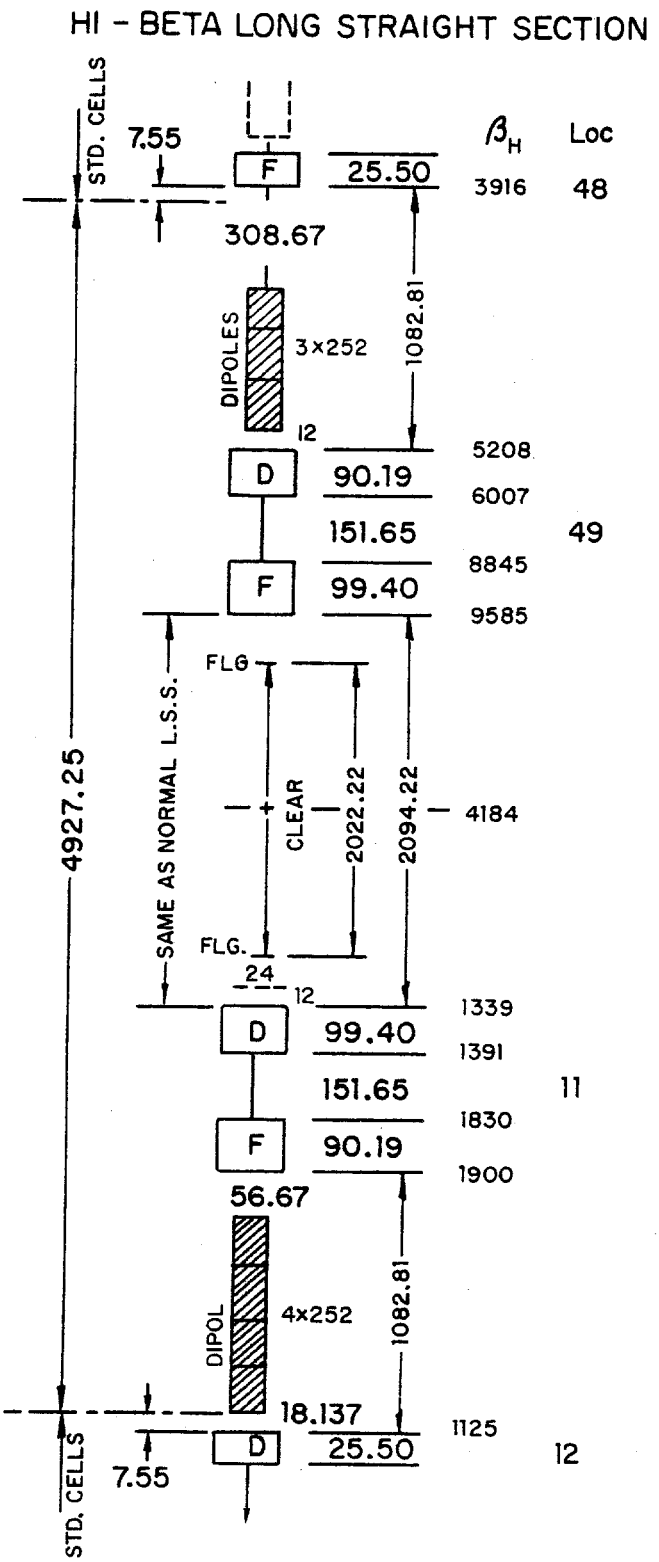

All dimensions in inches

Dipoles in slot length

Quads in eff. gradient length

Note: D-F order is not normal

Effective phase advance for hi-beta section is 112.12°

Hi-beta sector = long st. + 31 half cells $\phi = 83.11^{\circ}$

Ring = 2 hi-beta sectors + 4 normal sectors

$\nu = 19.4$

Figure 8-5 High-beta long straight section.

for the low-beta are listed in Table 8-III. A layout of the magnet elements of the low-beta straight section is shown in Fig. 9-1.

TABLE 8-III LOW-BETA QUADRUPOLES

Element	Magnetic Length (In.)	Number
Outer quadrupole(48,12 location)	66.1	2
	144.0	6
Inner quadrupole	180.0	2

8.3 Correction Systems

8.3.1 Types of Correction Elements. The correction magnets are built as a cluster of three functionally different superconducting coils concentric with one another and with beam-tube center line.[4] Since it was chosen to mount the coils on the cold beam pipe, or spool piece, between the quadrupole and the adjacent dipole in each cell, the correction magnet package is now called a spool piece. There are two basic types of spool pieces, the regular spool piece associated with each regular cell quadrupole, and the others. The distinction arises from the fact that each regular spool piece has two clusters of magnets, while the others have only one cluster of magnets. The upstream cluster of regular spool pieces contains dipole, sextupole, and quadrupole windings and the downstream cluster contains octupole, sextupole, and quadrupole windings. The orientations of the dipole winding and the downstream sextupole and quadrupole windings provide further differentation of the types of spool piece. The shorter spool pieces also contain three coils. Altogether there are seven types of spool pieces. The types of coils on each spool piece are given in Table 8-IV. The designations for the type of coils are as follows; horizontal dipole (H), vertical dipole (V), sextupole (S), quadrupole (Q), skew quadrupole (SQ), skew sextupole (SS), and octupole (E). Table 8-IV lists the types of spool pieces and Tables 8-IVa and 8-IVb give coil dimensions and parameters.

TABLE 8-IV ENERGY SAVER SPOOL PIECES

Spool piece Type (Code)	Upstream (DSQ coils)	Downstream (OSQ coils)	Length (in.)
"A"	H, S, Q,	None	43
"B"	V, S, Q	None	43
"C"	H, S, Q	E, SS, SQ	72
"D"	V, S, Q	E, SS, SQ	72
"E"	H, S, Q	E, S, Q	72
"F"	V, S, Q	E, S, Q	72
"G"	H, S, Q	E, S, SQ	72
"H"	H, V, SQ	None	50

TABLE 8-IVa DC MAGNETIC PARAMETERS OF CORRECTION ELEMENT COIL ASSEMBLIES

Package	Coil	T(bare) (G) (a)	Iron Factor	T(iron) (G) (a)	Effective Length (in.)(b)	$\int$Bdl at 50A and 1" (kG-in.)	Inductance (mH) warm bare(c)	cold iron(d)	cold iron(e)
DSQ	Dipole	89.20	1.466	130.80	27.69	181.10	475	696	686
	Sext	32.25	1.259	40.60	28.31	57.46	462	582	556
	Quad	31.67	1.662	52.63	28.56	75.16	293	487	479
OSQ	Octu	21.76	1.054	22.94	28.88	33.12	198	209	198
	Sext	24.51	1.281	31.39	28.32	44.45	300	384	370
	Octu	31.76	1.662	52.63	28.56	75.16	293	487	479

(a) Gauss at 1"/amp.

(b) Average of outer and inner coil lengths.

(c) Based on inductance-bridge measurements before installation of Al pipe.

(d) Base value x iron factor.

(e) Allowance for screening effect of superconductor.

TABLE 8-IVb PHYSICAL PARAMETERS OF CORRECTION ELEMENT COIL ASSEMBLIES

Package (a)	Coil	Coil inner radius (in.)	Coil outer radius (in.)	Iron inner radius (in.)	θ_{min} (b)	θ_{max} (b)	Coil inner length (in.)	Coil outer length (in.)	Iron length (in.)	Total turns	Coil-end geometry N-end
DSQ	Dipole	1.602	1.814	2.504	0°	60°	25-3/8	30	30	1170 (2x585)	0
	Sext	1.854	2.142	2.504	0°	20°	26-5/8	30	30	1965 (3x655)	2
	Quad	2.182	2.335	2.504	0°	30°	27-1/8	30	30	1240 (4x310)	0
OSQ	Octu	1.602	1.870	2.504	0°	15°	27-3/4	30	30	1500 (4x375)	2
	Sext	1.910	2.142	2.504	0°	20°	26-5/8	30	30	1560 (3x520)	2
	Quad	2.182	2.335	2.504	0°	30°	27-1/8	30	30	1240 (4x310)	0

(a) Packages include either normal or skew coils depending on subclass spec.

(b) Half angles given for normal coil-angles chosen to concel 3^{rd} harmonic.

(c) Using coil-end geometry ω per Snowdon's definition (memo dated 10/24/80).

8.3.2 Correction Magnet Circuits. The current leads of each coil are separately brought out of the spool piece cryostat, thereby making it possible to excite each coil independently. As will be discussed later, the dipoles are individually excited in order to correct orbit dislocations locally. The sextupoles, quadrupoles, and octupoles are series connected in functional groups in order to adjust global properties such as the tune and chromaticity.

Tables 8-V, 8-VI, and 8-VII show the type of spool piece at each quadrupole location, by pairs of sectors. Superscripts designate the arrangement of the coils into global circuits. Coil windings that are not noted in those tables are not connected to power supplies, although this could be done if a need arose.

TABLE 8-V COIL CIRCUITS IN SPOOL PIECES IN SECTORS A AND D

Quad Loc.	Spool Type	Upstream Coils	Downstream Coils	Quad Loc.	Spool Type	Upstream Coils	Downstream Coils
11	"H"	H, V, SQ^4	----------	12	"D"	V	SS^3
13	"G"	H, S^f, Q	SQ^0	14	"D"	V, S^d, Q	SS^3
15	"A"	H, S^f, Q	--------	16	"D"	V, S^d, Q	SS^3
17	"C"	H, S^f, Q	SQ^0	18	"D"	V, S^d, Q	SS^3
19	"C"	H, S^f, Q	SQ^1	21	"B"	V, S^d, Q	--------
22	"C"	H, S^f, Q	SS^2, SQ^0	23	"D"	V, S^d, Q	E^4, SS^4
24	"C"	H, S^f, Q	SS^2, SQ^2	25	"B"	V, S^d, Q	--------
26	"C"	H, S^f, Q	SS^2, SQ^0	27	"D"	V, S^d, Q	E^4, SS^4
28	"C"	H, S^f, Q	SS^2, SQ^1	29	"B"	V, S^d, Q	--------
32	"C"	H, S^f, Q	SS^1, SQ^0	33	"D"	V, S^d, Q	E^4
34	"C"	H, S^f, Q	SS^1, SQ^2	35	"B"	V, S^d, Q	--------
36	"C"	H, S^f, Q	E^3, SS^1, SQ^0	37	"D"	V, S^d, Q	E^4, SS^4
38	"C"	H, S^f, Q	SS^1	39	"B"	V, S^d, Q	--------
42	"C"	H, S^f, Q	E^3, SQ^0	43	"D"	V, S^d, Q	SS^4
44	"C"	H, S^f, Q		45	"B"	V, S^d, Q	--------
46	"C"	H, S^f, Q	SQ^0	47	"D"	V, S^d, Q	
48	"A"	H	--------	49	"H"	H, S^d, V, SQ^4	

TABLE 8-VI COIL CIRCUITS IN SPOOL PIECES IN SECTORS B AND E

Quad Loc.	Spool Type	Upstream Coils	Downstream Coils	Quad Loc.	Spool Type	Upstream Coils	Downstream Coils
11	"H"	H, V, SQ^4	--------	12	"D"	V	
13	"C"	H, S^f, Q	SQ^0	14	"D"	V, S^d, Q	
15	"A"	H, S^f, Q	--------	16	"D"	V, S^d, Q	
17	"C"	H, S^f, Q	E^1, SQ^0	18	"D"	V, S^d, Q	
19	"E"	H, S^f, Q	E^1, Q^1	21	"B"	V, S^d, Q	--------
22	"C"	H, S^f, Q	E^2, SQ^0	23	"F"	V, S^d, Q	E^4, Q^2
24	"E"	H, S^f, Q	E^2, Q^3	25	"B"	V, S^d, Q	--------

26	"C"	H, S^f, Q	E^1, SQ^0	27	"F"	V, S^d, Q,	E^4, Q^4
28	"E"	H, S^f, Q	E^1, Q^1	29	"B"	V, S^d, Q	--------
32	"C"	H, S^f, Q	E^2, SQ^0	33	"F"	V, S^d, Q	E^4, Q^2
34	"E"	H, S^f, Q	E^2, Q^3	35	"B"	V, S^d, Q	--------
36	"C"	H, S^f, Q	E^3, SQ^0	37	"F"	V, S^d, Q	E^4, Q^4
38	"C"	H, S^f, Q		39	"B"	V, S^d, Q	--------
42	"C"	H, S^f, Q	E^3, SQ^0	43	(D)	V, S^d, Q	
44	"C"	H, S^f, Q		45	"B"	V, S^d, Q	--------
46	"C"	H, S^f, Q	SQ^0	47	(D)	V, S^d, Q	
48	"A"	H	--------	49	"H"	H, V, SQ^4	

TABLE 8-VII COIL CIRCUITS IN SPOOL PIECES IN SECTORS C AND F

Quad Loc.	Spool Type	Upstream Coils	Downstream Coils	Quad Loc.	Spool Type	Upstream Coils	Downstream Coils
11	"H"	H, V, SQ^4		12	F	V	S^3
13	"C"	H, S, Q	SQ^0	14	"F"	V, S, Q	S^3
15	"A"	H, S, Q	--------	16	"F"	V, S, Q	S^3
17	"C"	H, S, Q	E^1, SQ^0	18	"F"	V, S, Q	S^3
19	"E"	H, S, Q	E^1, Q^1	21	"B"	V, S, Q	--------
22	"C"	H, S, Q	E^2,S^2,SQ^0	23	"F"	V, S, Q	E^4,S^4,Q^4
24	"E"	H, S, Q	E^2,S^2,Q^3	25	"B"	V, S, Q	--------
26	"G"	H, S, Q	E^1,S^2,Q!0	27	"F"	V, S, Q	E^4,S^4,Q^4
28	"E"	H, S, Q	E^1,S^2,Q^1	29	"B"	V, S, Q	--------
32	"G"	H, S, Q	E^2,S^1,SQ^0	33	"F"	V, S, Q	E^4,Q^2
34	"E"	H, S, Q	E^2,S^1,Q^3	35	"B"	V, S, Q	--------
36	"G"	H, S, Q	E^3,S^1,SQ^0	37	"F"	V, S, Q	E^4,S^4,Q^4
38	"E"	H, S, Q	S^1	39	"B"	V, S, Q	--------
42	"C"	H, S, Q	E^3,SQ^0	43	"F"	V, S, Q	S^4
44	"C"	H, S, Q		45	"B"	V, S, Q	--------
46	"C"	SQ^0		47	"D"	V, S, Q	
48	"A"	H	--------	49	"H"	H, V, SQ^4	

8.3.3 Coil Strength Requirements. The Q^f and Q^d quadrupoles are used to adjust the machine tune. There is a Q^f quadrupole adjacent to every regular horizontally focusing main quadrupole and a Q^d quadrupole next to every vertically focusing main quadrupole. The Q^f quadrupoles are connected in one series circuit, and the Q^d quadrupoles are connected in another. The S^f and S^d sextupoles are also designated in the same way by the adjacent main quadrupole. The S^f and S^d circuits are used to adjust the chromaticity.

The remaining correction magnets can be used initially for half-integer resonant extraction. The Q^1 and Q^3 circuits can be used for half-integer extraction, the Q^2 and Q^4 circuits can be used in conjunction with the Q^1 and Q^3 circuits to correct the $2\nu_x = 39$ and $2\nu_y = 39$ resonances. The 48 skew quadrupoles located in standard cells, SQ^0, are

connected in series. These are used to compensate the difference resonance, $\nu_x - \nu_y = 0$. If needed, skew quadrupoles at the ends of the long straight sectors, SQ^3, can also be excited to provide additional compensation of the $\nu_x - \nu_y = 0$ resonance.

The circuits SQ^1 and SQ^2, when powered, can be used to manipulate the half-integer sum resonance $\nu_x + \nu_y = 39$. The circuits S^1, S^2, S^3, and S^4, when powered, can affect the driving terms of the $3\nu_x$ and $\nu_x + \nu_y$ resonance should the need arise. Similarly, the skew sextupoles SS^1, SS^2 SS^3, and SS^4 are installed at the locations given in the tables for driving the $2\nu_x + \nu_y$ and $3\nu_y$ resonances.

Octupoles are arranged in four circuits. Circuits E^1 and E^2 provide the two phases of the 39th harmonic for resonant extraction. Circuits E^3 and E^4 produce the zero-harmonic nonlinearity for control of tune versus betatron-oscillation amplitude. The strengths of the coils appropriate for 1 TeV are expressed as field integrals at 1 in. radius.

Steering Dipoles. The primary function of the steering dipoles is the correction of the closed orbit at all energies. The rigidity of the superconducting-magnet system and the tight tolerance on orbit centering imposed by extraction rules out the movement of magnets for orbit correction. In order to make efficient use of the available magnet aperture, it was specified that the closed-orbit excursions be limited to ± 0.1 in. during extraction. This requirement is met by using the steering dipoles. The steering-dipole strength was determined to be 170 kG-in. on the basis of the following analysis:

At points in the normal cells where the amplitude function is a maximum, the rms orbit distortion due to dipole field errors and quadrupole misalignments can be written as

$$< x^2 >^{1/2} \approx \frac{1}{4}(a^2 + \frac{5}{9}b^2)^{1/2} \text{ in.}, \qquad (8.1)$$

Here a denotes the rms dipole field error in units of 0.1%, and b the rms quadrupole misalignment in units of 0.01 in. In the horizontal plane, a arises from the fluctuation in the field-length product from dipole to dipole. In the vertical plane, a receives contributions from both rotational alignment error and any uncertainty or instability in the dipole field direction. It was assumed that the typical misalignment error introduced into the orientation of the dipole vertical plane during installation was 1 mrad and the stability of that of the vertical plane also had an error of 1 mrad. It was assumed that the quad placement accuracy was 0.02 in. This leads to an rms closed-orbit distortion of 0.5 in. The dipole strength required to compensate the deflection generated locally by the quadrupole misalignment and by the 8 neighboring main dipoles, is, for uncorrelated dipole errors

$$(\int Bd\ell)_{rms} = 23(a^2 + 0.31b^2)^{1/2}\ \text{kG/in.}, \qquad (8.2)$$

where a and b have the same significance as in the previous expression. The assumptions made for alignment in the previous paragraph require a 41 kG/in. field integral to correct the rms error. For Gaussian errors, a steering strength of about 130 kG/in. is needed to have 90% probability of successful correction at 100 locations. The steering dipole was designed for a strength of 170 kG/in. This was considered adequate to meet the concerns of the preceding paragraphs.

Trim quadrupoles. Since the main dipoles and quadrupoles are connected in series, trim quadrupoles assume the burden of tune correction and adjustment. Appropriate quadrupole harmonic terms are needed for half-integer extraction.

One of the main functions of the trim quadrupoles is to compensate for the large incremental increase in tune caused by the low-beta interaction regions used in colliding beams. A typical interaction-region introduces an added betatron phase advance of close to 180° in both planes of oscillation. The trim quadrupoles must, in effect, lower both tunes by approximately 0.5 to restore the operating point. The B0 design described in Chapter 9 produces a shift in tune of 200°. The required trim-quadrupole strength at 1000-GeV may be inferred from

$$\begin{aligned} \Delta\nu_H &= 0.0214(B'\ell)_F - 0.0062(B'\ell)_D \\ \Delta\nu_V &= -0.0062(B'\ell)_F + 0.0214(B'\ell)_D \end{aligned} \qquad (8.3)$$

The subscripts indicate the focusing character in the horizontal plane of the adjacent quadrupole. A reduction of both tunes by 0.5 requires a contribution to trim quadrupole strength of 33 kG/in.

Tune corrections that must be made to compensate for magnet errors require considerably smaller strengths. A systematic quadrupole term b_1 in the dipoles would produce tune shifts $\pm 1.1\times 10^{3} b_1$ in the two planes of motion. On the basis of the production of 764 dipoles, the average value of b_1 is less than 10^{-5}/inch. This b_1 makes an inconsequential demand on the trim-quad strengths.

The trim-quadrupole strength was specified at 60 kG/in., safely above the requirement imposed by a single interaction region after allowance for tune correction. In order to operate two interaction regions, somewhat greater strength is required. The quad can be excited to higher currents if necessary, although a special supply is required. Alternatively, the operating point of the collider can be shifted from 19.4 to 19.6 to allow a greater tuning range.

Sextupoles. The principal role of the sextupoles is control of the chromaticity. At the time of the Superconducting Acceleration Design

Report, May 1979, high-field sextupole moments were cause for concern because b_2 was large. On the basis of the production of 764 magnets, the average value of b_2 is measured to be $10^{-4}/in^2$. As the following analysis shows b_2 is no longer a cause for concern.

The contributions to the chromaticity from systematic sextupole terms in the dipoles and from chromatic aberration in the quadrupoles can be written as

$$\xi_H = 2.64\times10^5 < b_2 > -22$$
$$\xi_V = -2.45\times10^5 < b_2 > -22, \qquad b_2 \text{ in } (\text{in.})^{-2} \qquad (8.4)$$

The constant value of -22 is due to the natural chromaticity of the basic lattice exclusive of enhancements from colliding-beam interaction regions. The magnet-selection criteria imposed a bound of 6.0×10^{-4} $in.^{-2}$ on the magnitude of b_2. The measured average value of b_2 leads to a chromaticity in one plane or the other of about 50. Compensation of this effect requires sextupole strengths of 4.5 and 1.5 kG/in. at horizontally focussing and defocussing quadrupoles respectively.

A colliding-beam interaction region can be expected to increase the natural chromaticity. For example: the design presented in Chapter 9 increases the magnitude of the chromaticity by 9 units, to -31. The sextupole associated with the standard-cell quadrupole was designed to have a strength of 50 kG/in., a value which is conservatively beyond the minimum requirements.

Octupoles. The major purpose of the octupoles is to facilitate resonant extraction. They provide the nonlinearity that divides the phase plane into stable and unstable regions for the case of half-integer extraction. On the basis of the requirements for resonant extraction, the individual octupole strength has been specified as 30 kG/in.

Skew quadrupoles. At an early stage of the operation of the Main Accelerator at high energy, it was observed that a large horizontal oscillation would couple over into the vertical in a single turn. On the basis of magnet measurements, the same thing occurs in the Energy Saver. For that reason, skew quadrupoles were incorporated into the spool pieces as noted in Tables 8-V, 8-VI, and 8-VII. The skew quadrupole is similar in all respects to the trim quadrupole except that it is rotated by 45°. It has the same strength of 60 kG/in.

8.3.4 Excitation. In this section, the tolerances on the currents delivered to the correction and adjustment magnets and their arrangement in circuits are discussed. The coils were specified to achieve their nominal design strengths at a current of 50 A. The coils can be separately powered at much higher currents. As noted earlier the circuits for exciting the coils are given in Tables 8-V, 8-VI, and 8-VII.

Current Tolerances. Because of their role in orbit correction, the steering dipoles inherently require independent bipolar power supplies. Stability and ripple suppression at 0.1% of full scale are sufficient to satisfy the demands of injection and extraction. Each of the global circuits, defined in 8.3.2, is powered by a precision supply which provides a current stability in the range of 0.1% to .005%. The most severe requirement these supplies must satisfy is to provide a relatively unmodulated resonant extraction over 10 seconds.

8.3.5 Power Supplies. Two distinct types of power supplies have been built, one with an accuracy of 0.1% in regulation for the steering dipoles, and a high precision supply for the other elements. There are 180 steering dipoles in the standard cells of the lattice, and at least 4 dipoles are installed at each long straight section.

The design value is ±50A. The supplies are designed with load compensation and a conventional roll-off characteristic of 20 db/decade.

Steering-Dipole Supplies. The current stability and ripple limit for these supplies is ±0.1% of full scale. To complete the specifications, the bandwidth and voltage must be determined. It is reasonable to have a bandwidth that allows the power supply output to follow a constant ramp input within ±0.1% of full scale. The error between programmed input and supply output for a constant ramp is

$$\varepsilon = \frac{AB}{2\pi f_o} \quad , \tag{8.5}$$

where ε is the lag error (amps), A is the power supply DC gain (amps/volt), B is the input voltage ramp rate (volts/s), and f_o is the power supply bandwidth or corner frequency (Hz)

For an error of 0.1% (0.05A) and a ramp from 0 to 50 A in 10 s, a power supply bandwidth of 20 Hz is adequate. With this 20 Hz bandwidth, the equation above then yields a maximum output ramp rate for 0.1% accuracy of 6.3 A/s.

The supplies are installed in the existing Main-Ring service buildings. The longest lead from the supply to dipole and back is 1200 ft. At 50A and 35°C, the voltage drop in that length of No. 1 wire is 8.1 V. The load inductance is approximately 0.7 H; at the maximum ramp rate, for 0.1% accuracy, the drop across the magnet would be 4.4 V. A maximum power-supply output of 15 V satisfies these requirements and provides a higher slewing capability for current changes under conditions where the accuracy specification can be relaxed.

A block diagram of such a supply is shown in Fig. 8-6. The control system provides a bipolar analog reference waveform from a generator with

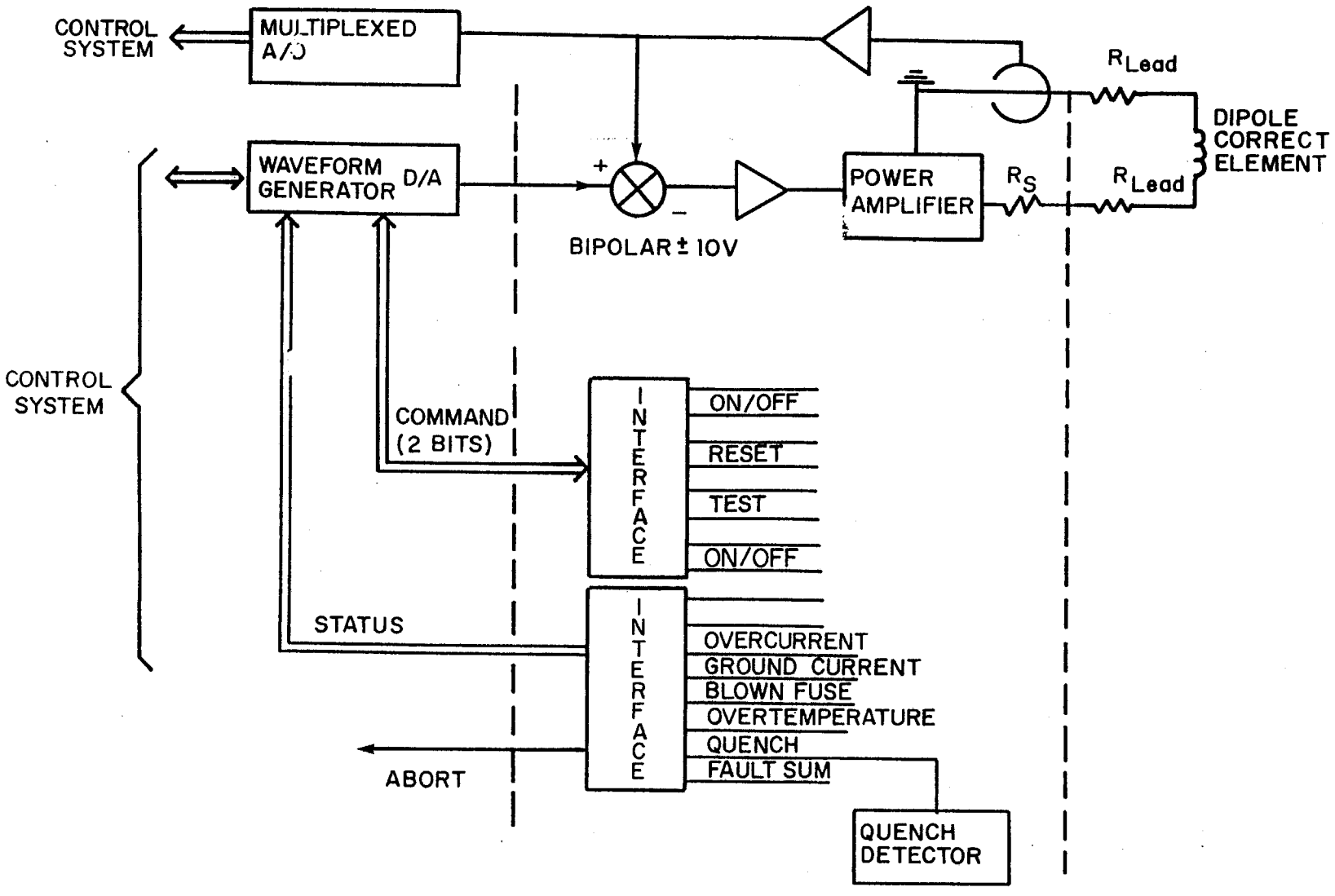
CONTROL SYSTEM
MULTIPLEXED A/D
WAVEFORM GENERATOR D/A
+
−
BIPOLAR ± 10V
POWER AMPLIFIER
R_S
R_{Lead}
R_{Lead}
DIPOLE CORRECT ELEMENT
CONTROL SYSTEM
COMMAND (2 BITS)
INTERFACE
ON/OFF
RESET
TEST
ON/OFF
STATUS
INTERFACE
OVERCURRENT
GROUND CURRENT
BLOWN FUSE
OVERTEMPERATURE
QUENCH
FAULT SUM
ABORT
QUENCH DETECTOR

Figure 8-6

12 bit resolution and 2 bits for commands to operate. The current reading is returned to the control system via a multiplexed A/D along with 8 status and fault bits. Isolation is provided between the control system and the power supply for command, status, and faults by means of optical couplers. Isolation of the analog signals is accomplished through differential drivers and receivers.

High-Precision Supplies. These supplies have a stability and ripple limit in the range 0.005% to 0.01% of full scale current. They are rated at ±50A, ±600V. The low ripple current is achieved with a bipolar transistorized output regulator.

It is noted that certain of these supplies have a relatively high output voltage. To reduce transistor-bank dissipation, these supplies use a bipolar SCR preregulator to provide variable voltage to the output transistor regulator. The preregulators are adjusted to keep a nearly constant voltage across the output transistor banks and thus reduce the transistor-bank requirements. The transistor-bank regulators for the various high-precision supplies are essentially the same. The same is true of the preregulator.

The reference voltage is provided by a high precision 16 bit D/A and the current sensor is a high-quality current transductor with a stability of 1 ppm/°C. The waveform generator is located within the supply to minimize noise pickup. Quench detection is also provided by comparing the voltage across one half the series regulators to the other half.

8.4 Main Ring Extraction and Energy Saver Injection and Abort

The design of the antiproton beam transfer was simplified considerably once the circumference of the Energy Saver was made equal to the Main Ring. Fig. 8-7 is a schematic representation of the E0 straight section, which shows both the proton and antiproton transfer lines.

Proton injection for colliding beams will proceed with the transfer of a single bunch from the Main Ring to the Tevatron. The bunch will be kicked horizontally across a magnetic septum (Lambertson magnets) in the Main Ring at the upstream end of E0 using the existing extraction kicker magnet at C48. This initiates a downward bend (16.6 mrad) towards the superconducting string at E11, 25.5 in. below the Main Ring. The vertical dog-leg is completed by two more Lambertson magnets at the downstream end of the long straight section, which brings the beam back on to the horizontal plane. The beam is then placed on the closed orbit by another fast rise-time kicker magnet located at the warm E17 medium straight in the Tevatron. Although the basic lattice structures of the Main Ring and the Tevatron are similar, a transverse-emittance dilution of approximately 30% would occur if no attempt were made to match the beam shape. A quadrupole in the injection line will be used to provide both horizontal and vertical matching. Horizontal beam steering is accomplished in the Main Ring and the injection line by a series of bump magnets; the correction dipoles accomplish the corresponding function in the Tevatron.

INJECTION LINE SCHEMATIC (VERTICAL)

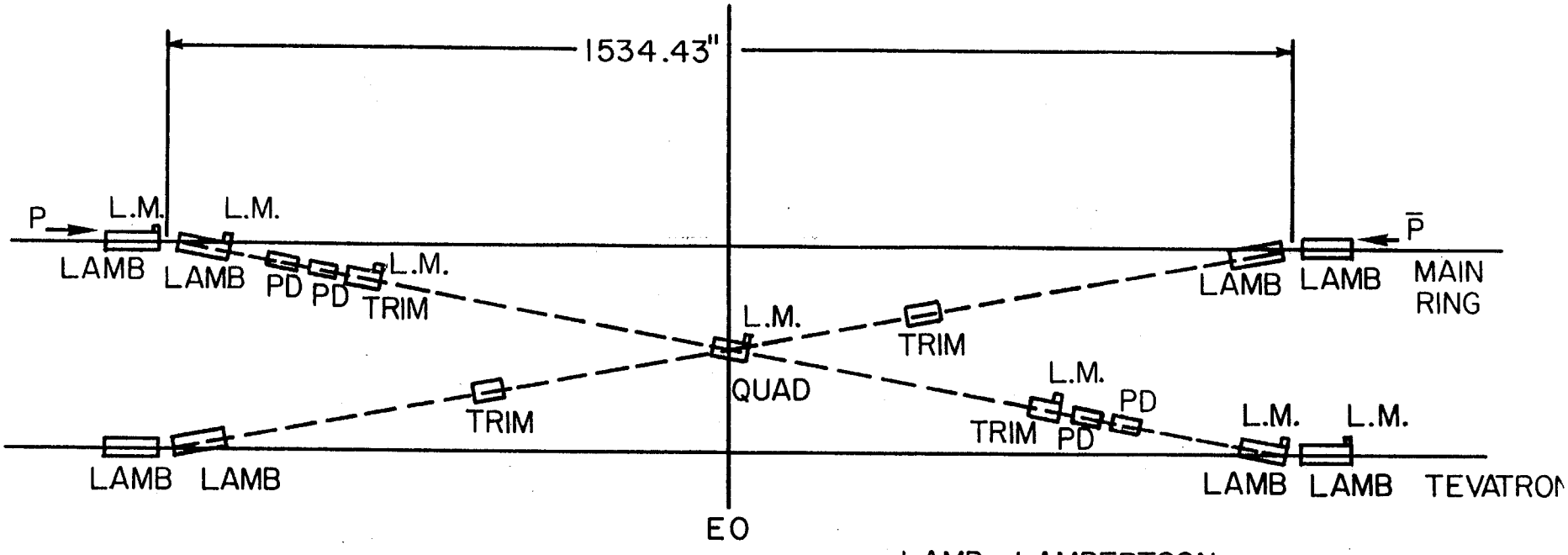

LAMB - LAMBERTSON

P.D. - POSITION DETECTOR

L.M. - LOSS MONITOR

Figure 8-7

Antiproton injection uses four additional Lambertsons and two trims, as shown in Fig. 8-7. The matching quad is common to both lines. The $\bar{p}$ transfer is accomplished in a similar manner as for protons with the Main Ring extraction kicker located at E17 and the saver injection kicker located at D48.

Table 8-VIII lists the kicker requirements for six bunches of protons and six bunches of antiprotons, all equally spaced. This establishes the maximum number of bunches that can be injected. Nevertheless, it is not planned to exceed 3 bunches of protons and 3 bunches of antiprotons at this time. The specifications for the proton transfer kickers were set by the requirements for fixed-target operations.

The specifications listed in Table 8-VIII allow injection of either protons or antiprotons first. If the protons are injected first, either a single bunch at a time may be injected, or all three (or six) bunches may be injected together. The antiprotons are then interspersed among the proton bunches, one bunch at a time. However, the resulting collision points are then approximately 200 m from the 0 stations. Subsequent to injection, the collision points may be moved to the 0 stations using the orthogonal RF systems in the Tevatron. This operation involves non-head-on collisions (e.g., $\Delta R \sim 0.1$ mm) but is completed in such a short period of time (7 secs), that, on the basis of both, computer simulations and operational experience at CERN, no significant phase-space dilution due to the enhanced beam-beam interaction is expected.

Table 8-IX lists the requirements of the proton and antiproton abort kickers. The requirements for the proton abort kicker are met in the existing design for fixed-target application.

The $\bar{p}$ abort kicker requirements can be met by three 1.9 m long modules of the Main Ring abort style (tape-wound core). These kickers produce a ~25 mm displacement at the downstream end of the C0 straight section. A 10 feet long steel dump located at this point serves as the abort dump. This simple abort system suffices because of the low beam intensity in the $\bar{p}$ beam. The more complicated abort system for the protons has been designed for the two orders of magnitude more intense proton beams that is required for fixed-target operation.

The use of the C48 kicker to inject protons at E0 creates the possibility of introducing uncomfortably large amplitude oscillations through D sector of the Main Ring. In order to reduce the size of these oscillations where possible, three bump magnets have been installed in the Main Ring at C22, C32 and D38. These three magnets can be excited to produce a closed orbit 180° out of phase with the kicked beam and thus reduce the effective orbit excursions by a factor of 2 throughout most of the sector. Precise control of the beam position in the Main Ring across the long straight section, essential to ensure loss-free injection, is provided by another set of bump magnets at D46 and E17. Powered in series, these magnets generate an orbit bump similar to that currently used in the

MAIN RING CLOSED ORBIT
PRIOR TO INJECTION

HORIZONTAL PROJECTION
TUNE: 19.420
MAX. OFFSET: 2.34 cm

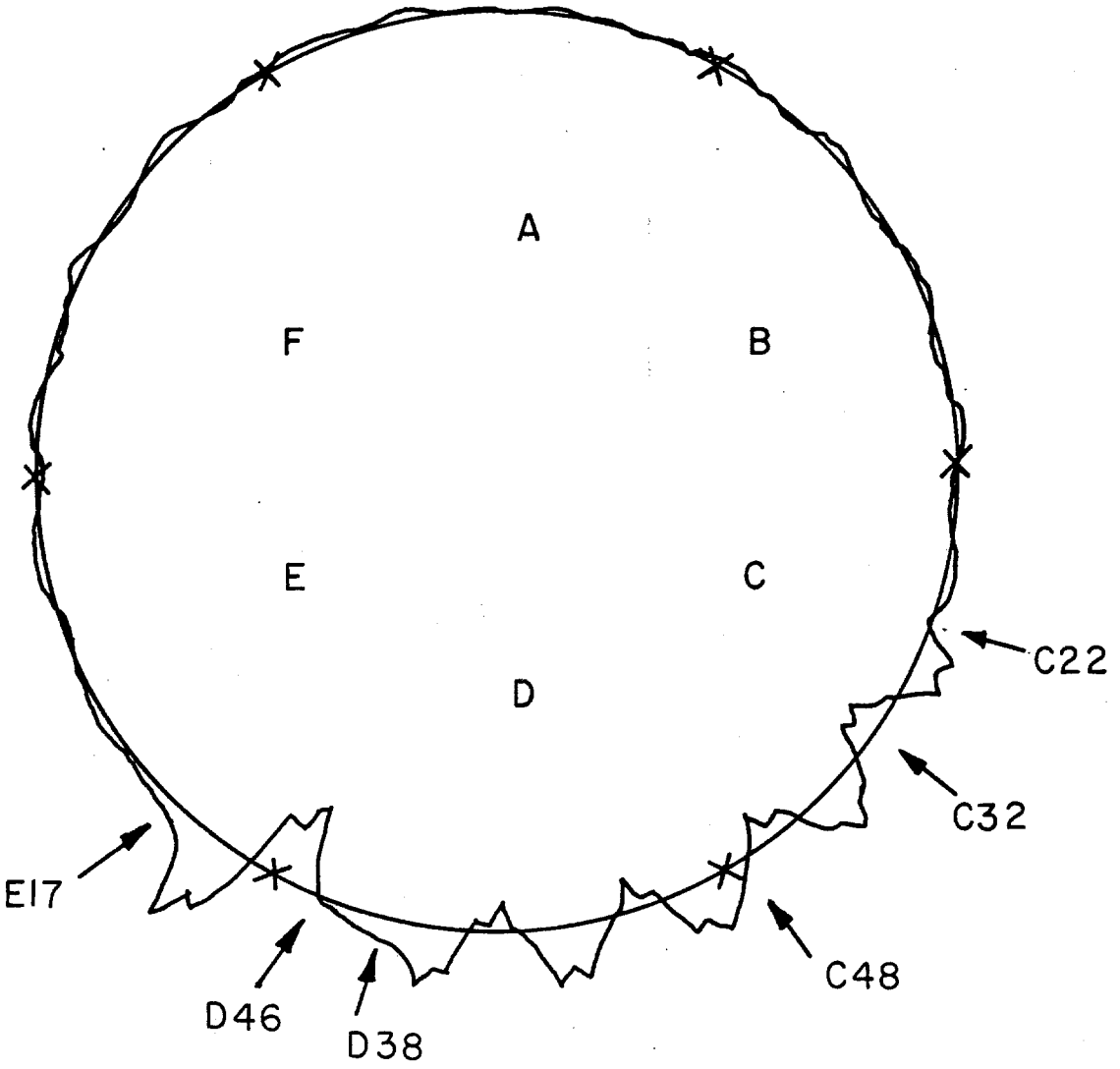

Figure 8-8

Main Ring for extraction. A hypothetical closed orbit suitable for injection is shown in Fig. 8-8. The orbit excursions between C22 and D38, D46 and E17 are apparent. Figure 8-9 shows the same closed orbit modified by firing the kicker that produces the orbit cusp at C48. The orbit amplitude remains approximately constant up to D38, after which the amplitude increases to a maximum offset of 48 mms at D48. The horizontal orbits across the long straight section are shown in more detail in Fig. 8-10a, where the error bars on the Main Ring orbits give the expected beam size (± 4 mm) at the Lambertson septum. With these injection parameters, one can see an intrabeam separation of 7 mm with the septum offset at 25 mm. The corresponding Tevatron orbits are shown in Fig. 8-10b. The closed orbit bump between E11 and E17 is generated by the correction coil dipoles at E11, E13, E15, and E17 and serves to reduce orbit excursions within the restricted aperture of the Tevatron as well as decrease the integrated field strength required from the kicker magnet at E17.

For $\bar{p}$ reverse transfer, the 046-E17 Main Ring bump magnets will be used for position control of the $\bar{p}$ beam at the reverse injection Lambertsons. Figure 8-11 shows the $\bar{p}$ extraction orbit in the Main Ring. The maximum expansion from the Main Ring center line is 35 mm at E15.

Figure 8-12 shows the $\bar{p}$ transfer line trajectory. The Main Ring Lambertson septa are at approximately 15 mm (relative to the Main Ring center line); the Tevatron Lambertson septa are at approximately 16 mm and approximately 8 mm (relative to the Tevatron center line). The relatively large injection angle shown in the figure is necessary because of the small phase advance between the injection point and the D48 kicker.

Horizontal correction dipoles at D48, D49, E11 and E13 will be used to control the beam position at the Lambertsons after injection.

The injection Lambertson magnets are similar in design to the present Main Ring extraction devices. The magnets have 12 turns of water-cooled 0.46"-square copper giving a useful dipole field aperture of 3.5" x 0.9". The nominal operation current of 1575 A produces a 9 kG field. The maximum useable field is defined by the saturation of the steel (Republic Steel LoCore 'B') and is 12 kG. The septum is 2 in. thick and is formed with a half angle of 45°.

TABLE 8-VIII EXTRACTION AND INJECTION MAGNET PARAMETERS

	p Extraction	p Injection	$\bar{p}$ Extraction	$\bar{p}$ Injection
B-ℓ	1.97 kG-m	1.5 kG-m	2.25 kG-m	5.2 kG-m
Rise time	20 μsec	1.39 μsec	11 μsec	1.5 μsec
Fall time	--	2.0 μsec	--	1.5 μsec
Magnets	6	2	1	2
Magnet impedance	25Ω	12.5Ω	5.5 Ω	5Ω
Magnet length (m)	1	2.1	1.9	2.1
No. of				

MAIN RING INJECTION ORBIT

HORIZONTAL PROJECTION

TUNE: 19.420

MAX. OFFSET: -4.82 cm

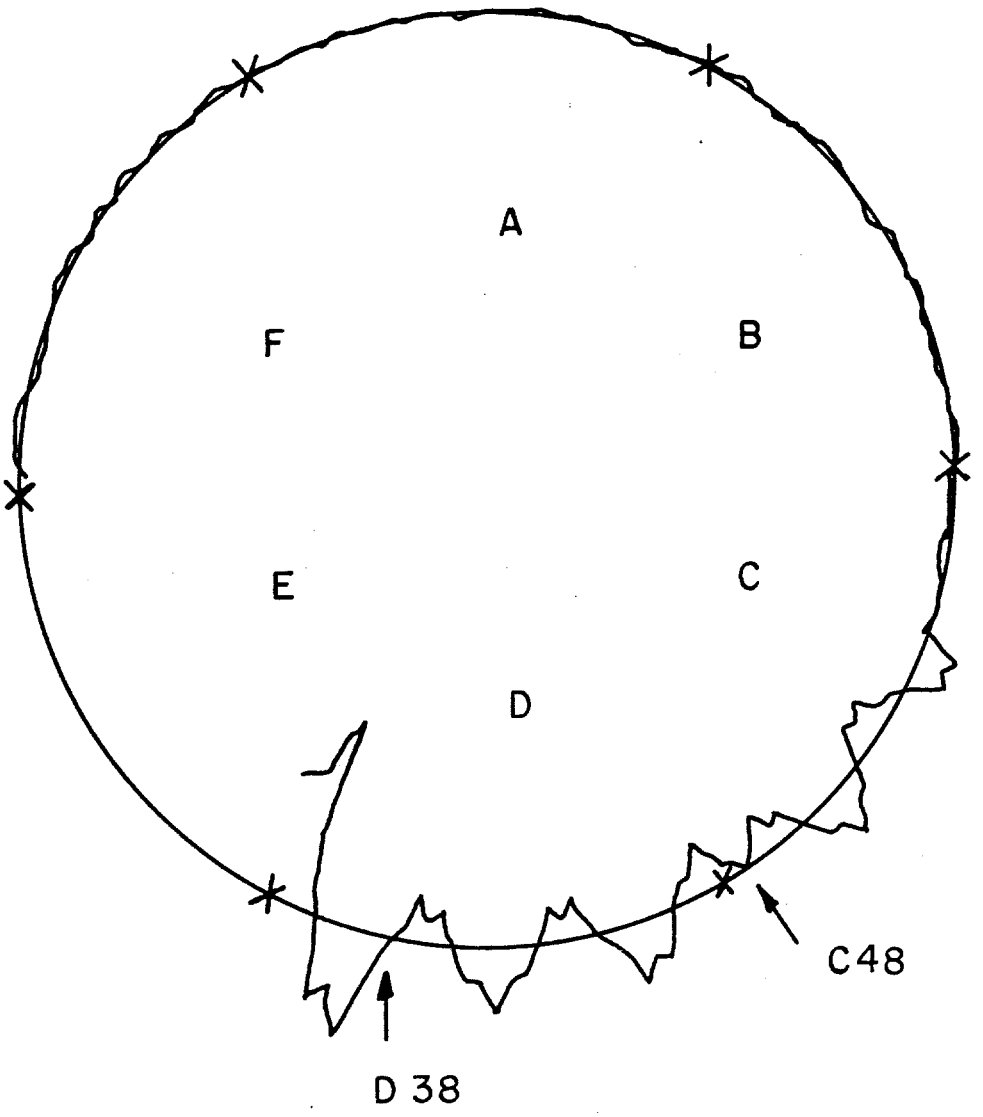

Figure 8-9

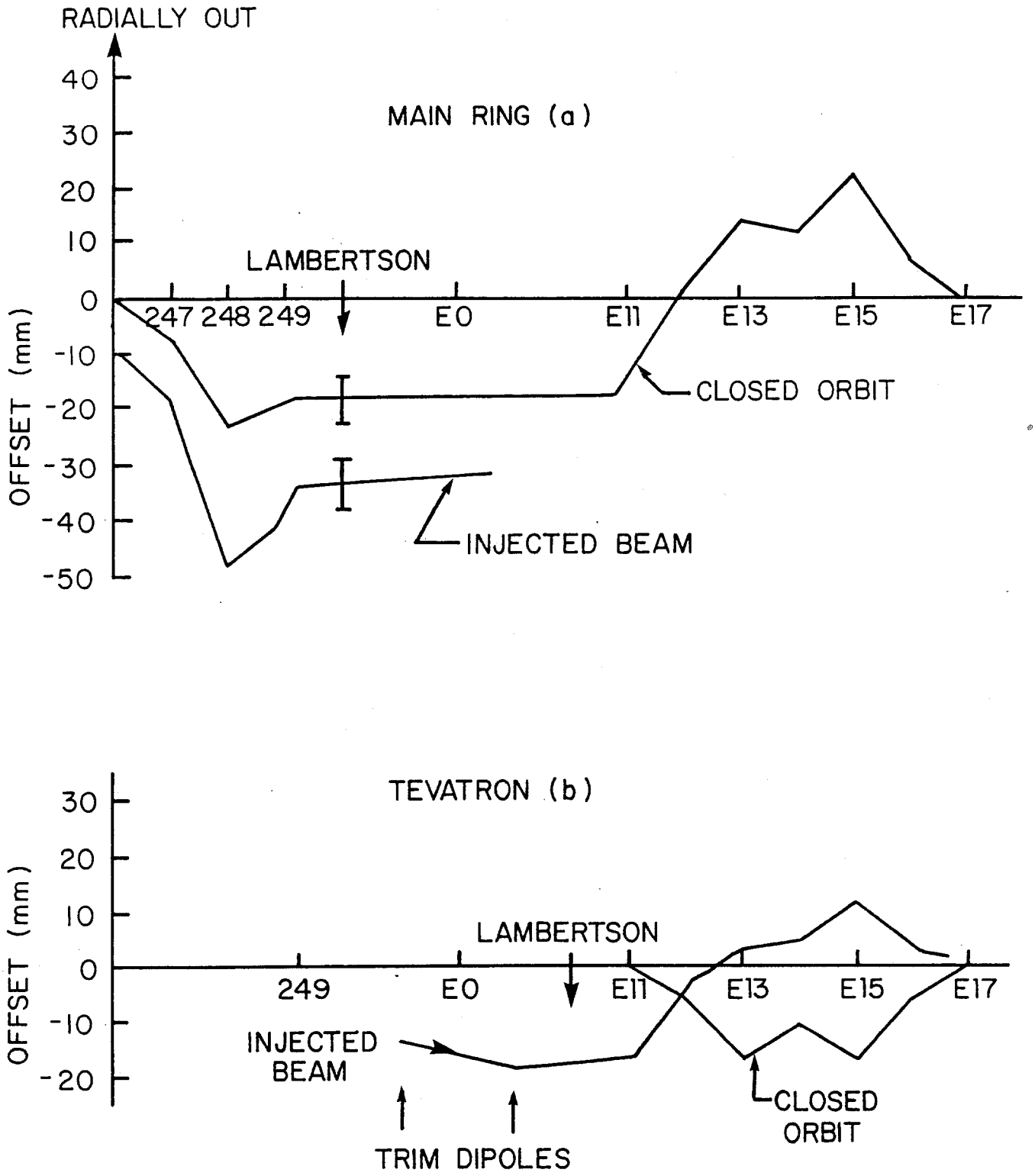
RADIALLY OUT
MAIN RING (a)
40
30
20
10
0
-10
-20
-30
-40
-50
OFFSET (mm)
LAMBERTSON
247 248 249
E0
E11
E13
E15
E17
CLOSED ORBIT
INJECTED BEAM
TEVATRON (b)
30
20
10
0
-10
-20
OFFSET (mm)
LAMBERTSON
249
E0
E11
E13
E15
E17
INJECTED BEAM
CLOSED ORBIT
TRIM DIPOLES

Figure 8-10

TUNE 19.400
MAX. OFFSET 3.5
HORIZONTAL PROJECTION

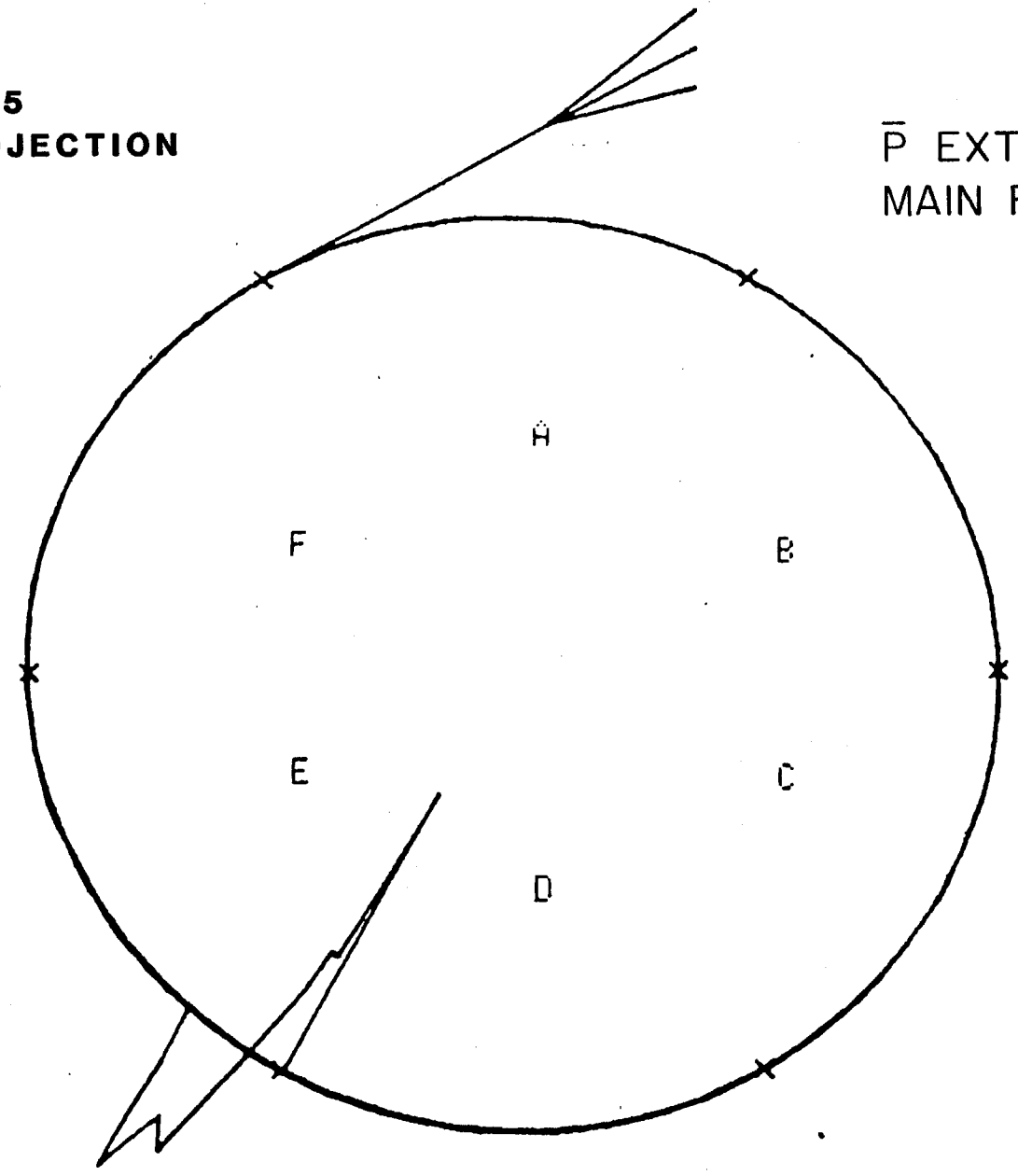

Figure 8-11

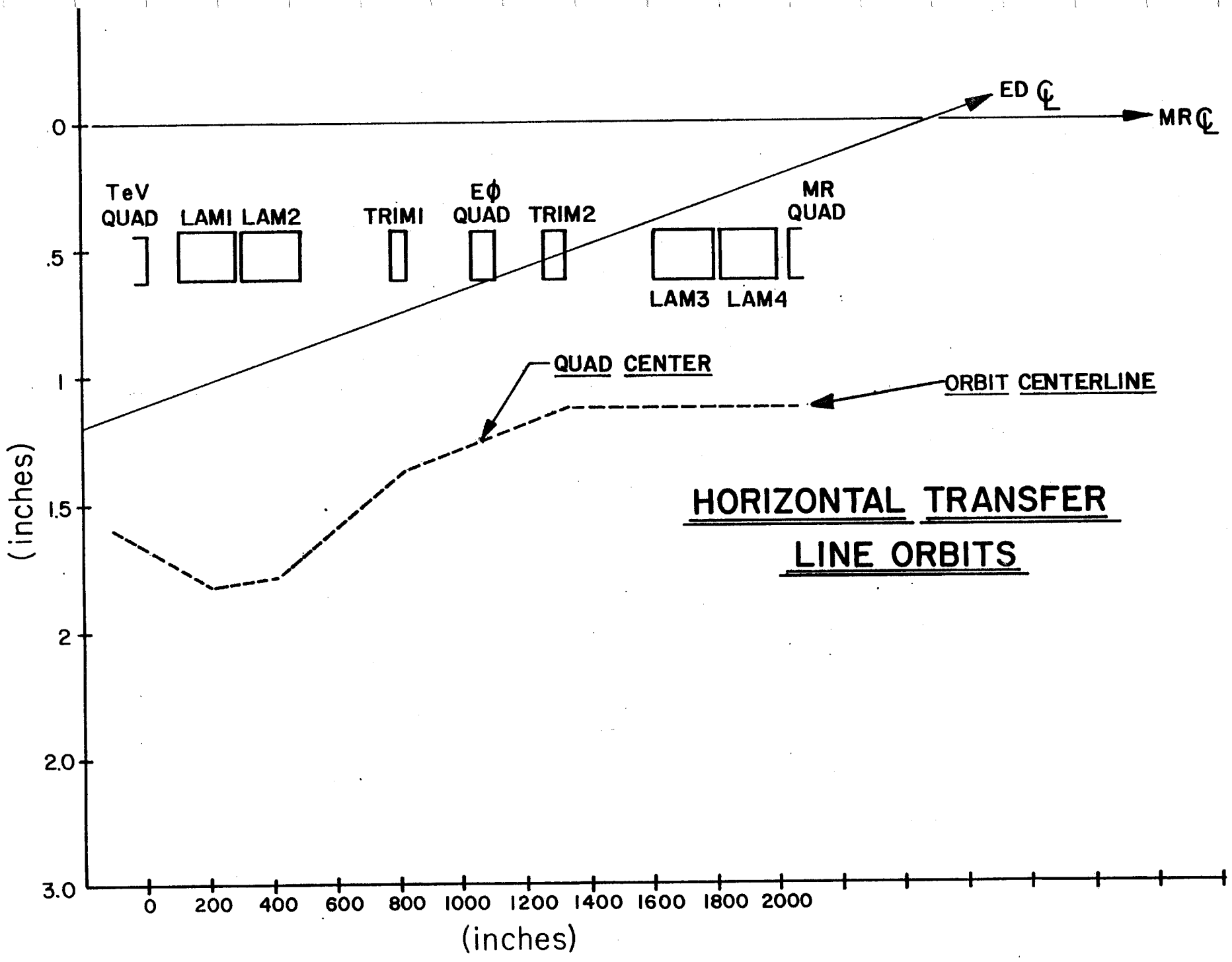
ED ℄
MR ℄
TeV QUAD
LAM1 LAM2
TRIM1
Eϕ QUAD
TRIM2
MR QUAD
LAM3 LAM4
QUAD CENTER
ORBIT CENTERLINE
HORIZONTAL TRANSFER LINE ORBITS
0
.5
1
1.5
2
2.0
3.0
(inches)
0 200 400 600 800 1000 1200 1400 1600 1800 2000
(inches)

Figure 8-12

pulse-forming networks	1	1	1	1
PFN impedance	12.5Ω	6.25Ω	1 Ω	2.5Ω
Gap (inches)				
HxV	6x2	2x2	3.4x1.5	2x2
Voltage	56 kV	43 kV	4 kV	50 kV

TABLE 8-IX ABORT MAGNET PARAMETERS

	P Abort	$\bar{p}$ Abort
B-ℓ	24 kG-m	15 kG-m
Rise time	1.6 μsec	2.0 μsec
Location	B-48	C-17
No. module	4	3
Length	2 m	2 m
I_{max}	19 kA	11 kA

8.5 Acceleration of Protons and Antiprotons

8.5.1 Energy Saver RF Requirements for Colliding Beams. When the Energy Saver is used for colliding beams, the rf system must be able to accelerate protons and antiprotons simultaneously from 150 to 1000-GeV. Because the longitudinal emittances of proton and antiproton bunches may be slightly different, it may be necessary to provide different bucket areas for each in order to minimize dilution during acceleration and storage. Dynamic phase adjustment of proton and antiproton buckets will be necessary in order to damp coherent dipole oscillations of the separate bunches. The rf system should also have the capability of moving the azimuthal location of the $\bar{p}p$ collision point. These functions can be satisfied if the rf system allows independent control of the amplitude and phase of the proton and antiproton buckets.

Independent control can be achieved by arranging the cavities in pairs with appropriate spacing and phasing. Consider a pair of cavities separated in space by $3/4\lambda$ ($\lambda=2\pi R/h$, the rf wavelength at $\beta=1$). If the phase of the rf voltage on the downstream cavity is advanced by $\pi/2$ radians the rf fields encountered by a particle moving downstream through the two cavities will be exactly in phase. These same fields are exactly out of phase for a particle moving from the downstream cavity to the upstream cavity.

There are eight Energy Saver rf accelerating cavities, each of which is capable of sustaining 35-GeV/sec accelerating voltage for colliding beam

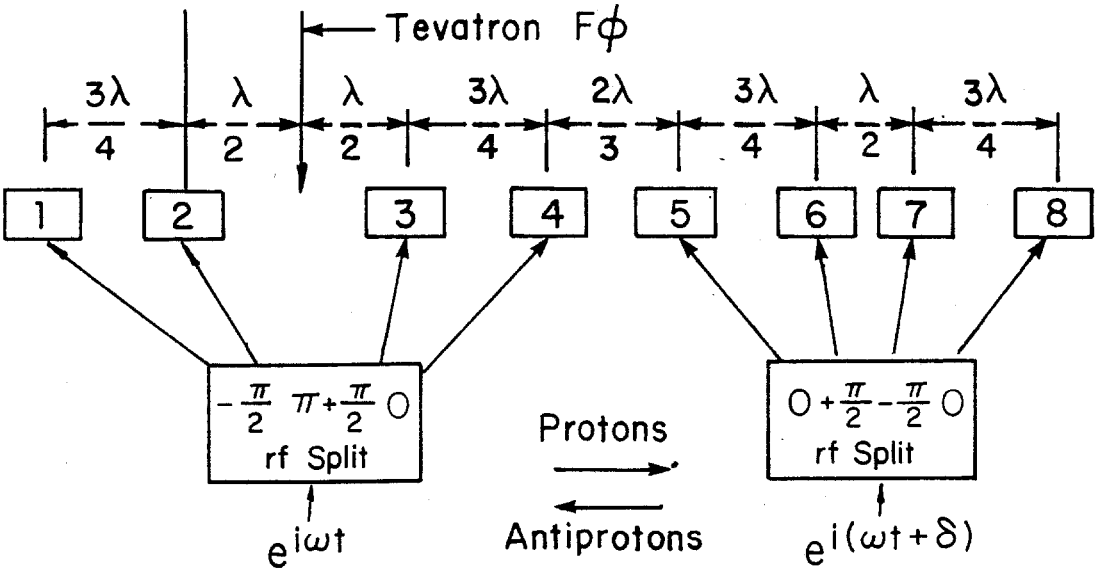

(a)

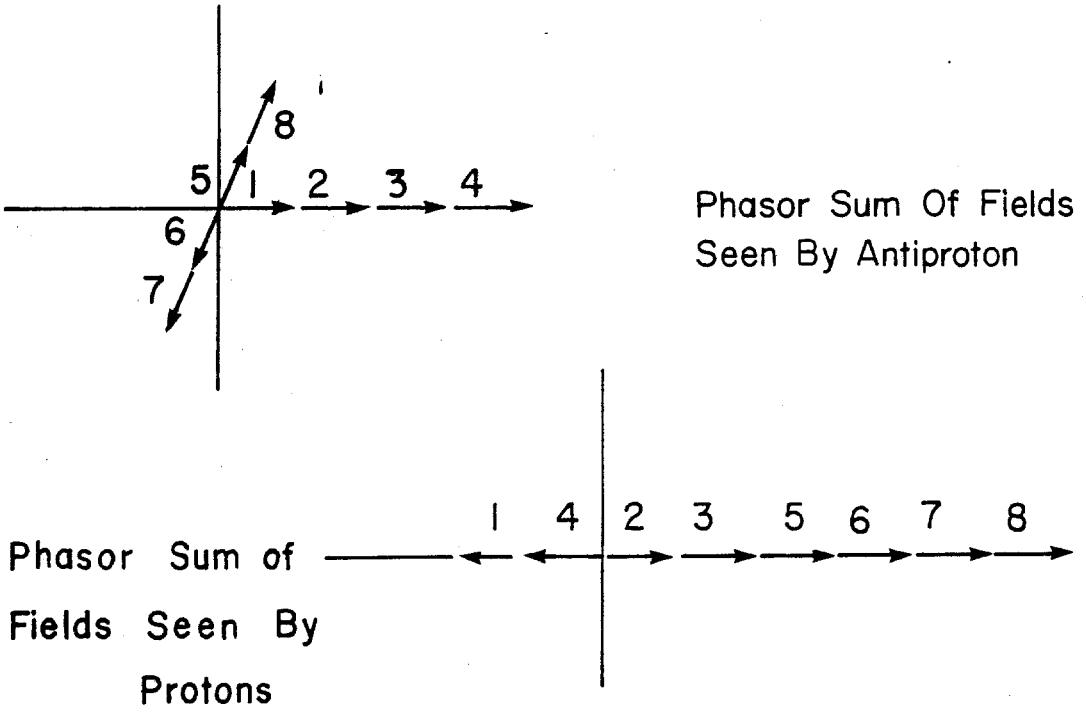

(b)

Figure 8-13

operations. Five of these cavities were built as part of Tevatron I. Four cavities are arranged in two pairs with a spacing of $3/4\lambda$ to accelerate protons and the remaining four will be arranged in two pairs with the same spacing to accelerate antiprotons as shown in Fig. 8-13a. Cavities 1, 2, 3, 4 are phased so that they couple to antiprotons, which move to the left. Cavities 5, 6, 7, 8 couple to protons, which move to the right. The center of cavity number 2 is located at the Tevatron F0 location. Since this location is symmetrically located with respect to the design collision points at D0 and B0, bunches that collide at those points must arrive at the F0 point at the same time (i.e., they collide there also, in the case where there are three bunches each of protons and antiprotons in the Collider). The arbitrary angle δ is adjusted to establish the correct collision pont. For the spacing shown the required value of δ is $\pi/6$ radians.

These cavities are adequate for an acceleration rate of 34 GeV/sec at a synchronous phase of 30°. The acceleration time to 1000 GeV is then 25 sec. The bucket size is ample. The relative phase between the two sets of cavities is adjustable, so that the $\bar{p}$ and p bunches can be rotated relative to each other to move the collision point to any desired azimuth.

8.5.2 Failure Modes. The requirement of orthogonal control of the two sets of cavities establishes uniquely the spacing between pairs of cavities. However, the precise location of the cavities and the selection of which set to assign to protons or antiprotons is arbitrary. The collision point can be adjusted by selection of arbitrary phase angles δ, as illustrated. The effect of the failure of a single cavity on beam size, luminosity and stability of the collision point is determined by cavity location and deployment. Failure of any rf cavity will always result in some beam deterioration, but the damage can be minimized by optimum cavity placement and selection.

The placement of cavities is partially limited by the location of penetrations and equipment in the RF Building and the F0 Straight Section. The cost of rearranging equipment did not always justify the gains that the optimum arrangement provided. The distribution described here is a partial optimization consistent with existing constraints.

In Fig. 8-13b the instantaneous fields seen by protons and antiprotons are shown. A failure of any one of the proton cavities, 5-8, would result in a sudden change in the phase and amplitude of the rf field seen by antiprotons. The antiproton bunches would immediately start a coherent dipole oscillation about the new phase angle, together with higher-order oscillations resulting from a change in bucket size. This would appear as an oscillation of the collision point and ultimately a dilution of the antiproton bunch length to cover the entire oscillation range. This dipole motion can be prevented by automatically turning off a second proton cavity so that the balance is restored. Removal of two proton cavities results in a reduction in bucket height by a factor of 0.707. This will cause a bunch

quadrupole oscillation with attendant dilution and bunch lengthening, but no dipole motion of the bunch or collision point.

On the other hand, failure of one of the antiproton cavities, 1-4, does not cause a phase displacement of the proton field, so no additional cavity need be removed from the system. Such a failure results in a decrease in the antiproton bucket height by a factor of 0.866 with a small attendant quadrupole oscillation and bunch lengthening. The effect on the proton bucket height and bunch length is to increase or decrease it by an even smaller factor. In summary, the cavity locations and assignments are such as to minimize the effect of failure of any cavity on the quality of the antiproton bunches at the expense in some cases, of proton bunch quality.

It is conceivable that if many faults occur, resulting in unacceptable dilution of proton bunches, both beams could be decelerated to 150 GeV and the proton bunches replaced with fresh ones while keeping the old antiproton bunches.

8.6 Energy Saver Diagnostics

At the time the Energy Saver components were fabricated, it was recognized that it would be used as a collider. For that reason the beam position detectors were designed so that the proton and antiproton beam could be detected simultaneously. Since the decision to build this type of monitor was made after the preparation of the Superconducting Accelerator Design Report, a description of them is given in Section 8.6.1. The beam-loss monitors of the Energy Saver are described in 8.6.2. Following the first year of operation of the SPS collider, the requirements for diagnostics in the Energy Saver were reviewed. The additional diagnostic equipment to be added to the Energy Saver for colliding beams is given in Section 8.6.3.

8.6.1 Energy Saver Position Detectors. The position detectors in the Tevatron are of the directional-coupler type[5]. There are 216 detectors in all, 108 each for vertical-position measurement (in vertical focusing quadrupoles) and for horizontal-position measurement (in horizontally focusing quadrupoles). The pickups have about 24 db of directivity (i.e. rejection of signals from beam traveling in the unwanted direction) so that the pickups can be used to detect $\bar{p}$'s in the presence of p's and vice versa.

The fast electronics for extracting the position signal from the pickup signal uses amplitude-to-phase (AM to PM) conversion to provide a large dynamic range of beam intensity[6]. The electronics was specifically designed to detect single isolated bunches of p's or $\bar{p}$'s (collider mode) as well as contiguous filled buckets (batch mode) for fixed-target operation. The lower limit of sensitivity for operation in these modes is about 3×10^9 p's per bucket (collider mode) or 1×10^8 p's per bucket (batch mode). The

position-signal rise time is about 70 nsec due to the presence of a half-wavelength resonant filter which rings when hit by a signal from isolated p or $\bar{p}$ buckets. The estimated precision of position measurement is about ±0.5 mm at the lowest intensities. Precision of ±30 microns has been obtained with high intensities in a detector installed in the Main Ring.

The microprocessor-controlled digitizing electronics allows simultaneously digitizing the position signal from all 216 detectors with about 100 nsec (least significant bit) resolution on the timing for each detector. This "FLASH" picture of a single turn of beam can be used to examine the beam orbit for any complete revolution including injection. Other operating modes include measurements of beam position averaged over many turns to average out the contributions of betatron oscillations. These latter measurements have large RAM memories associated with them to store many measurements without requiring readout by the Host control computer. These data are used to determine closed orbits for correction-coil programming and for orbit reconstruction in case of a beam-induced quench. The microprocessor circuits can initiate beam aborts if the beam exceeds preset position limits.

The electronics has been designed and built to detect beams in either direction. In order to fully implement these features, coaxial relays are installed in the tunnel to select the proper pair of ports from the directional coupler pickups. A signal to control them is provided in the Service Buildings. In addition, a Saver Clock signal (a signal with diphase encoded timing signals on a 10 MHz carrier) is installed in the $\bar{p}$ direction around the ring. The electronics is equipped to receive this at the same time it controls the coaxial relays. A control cable for the coaxial relays will also be installed.

8.6.2 Beam Loss Monitors. The Tevatron beam-loss monitor system, like the beam-position system has detectors at every quadrupole (a total of 216 around the ring). They are argon filled chambers designed to have a very large dynamic range and fast response. Their signals are amplified in a fast-risetime integrating 4-decade logarithmic readout. Real-time analog output signals are also available for fast time plots. The 60 msec integration time of the electronics corresponds to the response time of the Doubler magnets to beam-induced heating, and therefore is a good monitor of the likelihood of inducing quenches. The beam-loss monitor system, like the beam-position system, can initiate a beam abort if the radiation level exceeds preset limits.

8.6.3 Diagnostics for the Energy Saver Collider Operation. Initial experience from the CERN SPS collider has shown the importance of adequate beam diagnostics. In the Fermilab Collider, much of the tuning of the transfers, acceleration, and storage parameters will necessarily be done with antiprotons, which are relatively rare even if the $\bar{p}$ accumulation works well. Thus, diagnostic devices should work at low beam intensities.

Furthermore, since the time to improve transfer and storage efficiency of the Collider will be in competition with other uses of the Tevatron, there must be a complete set of diagnostic devices with well developed software at the onset of Collider commissioning.

The obvious requirement is to be able to measure the beam intensity, position and emittance as a function of time as the particles make their way to a successful store at 1 TeV.

Beam-transfer lines will be equipped with sensitive intensity and profile monitors. The Main Ring and Tevatron have position and intensity measuring devices that will be well developed by the time collider commissioning begins.

In order to measure the profile of circulating p's and $\bar{p}$'s in the Tevatron, we are constructing several flying wire scanners[7]. These devices flip a thin-wire filament through the circulating beam at about 5 m/sec, and the resultant scattered flux is monitored by several scintillator telescopes placed both upstream and downstream of the flying wire. Such a device will be placed near (and in) the B0 Colliding Detector Facility to measure beam position as well as profile. Each flying wire can measure only one coordinate, so several are needed. Such a device has been implemented at the CERN SPS and is recognized as an important diagnostic tool[8].

Motion of the wire through the beam is about 0.1 mm per turn, which results in about 10 points across a beam 1 mm in diameter. The scattered flux from p's and $\bar{p}$'s are quite directional, and hence the p and $\bar{p}$ beam profiles are recorded simultaneously in the two sets of scintillators. The emittance blowup per scan is about 6×10^{-6} mm-mrad, hence for the SPS about 200 scans per hour is equivalent to multiple scattering by the residual gas. The heating of the wire (a low-Z material such as beryllium or carbon) is not excessive. The particle flux lost is less than 0.02% per scan.

Longitudinal emittances will be monitored by the devices associated with the Main Ring and Tevatron low-level rf systems.

Schottky scans should be adequate for tune measurements. An active tune measurement is also under consideration.

The intensity and position devices in the Tevatron can give information on individual bunches of protons or antiprotons. In addition, the flying-wire scanner gives bunch-by-bunch information.

References

1. Superconducting Accelerator Design Report, May 1979, Fermilab, Chapter 14.
Fermilab Report UPC 73, F.E. Mills and D.E. Young, November 11, 1978.
Fermilab Report UPC 129, F.T. Cole, April 24, 1980
Fermilab Report UPC 132, S. Ohnuma, June 26, 1980

2. Fermilab Report UPC 96, T.L. Collins, April 1979.

3. Fermilab Report UPC 17, L.C. Teng, December 1, 1978

4. D. Ciazynski and P. Mantsch, "Correction Magnet Packages for the Energy Saver" IEEE Trans. on Nuclear Science, Vol. NS-28 , No. 3, 3275 (1981).
D. Ciazynski and P. Mantsch, "Typical Problems of Correction Magnets for Fermilab", IEEE Trans. on Magnets, Mag-17, 165 (1980).

5. R. Shafer et al., IEEE Trans. Nucl. Sci. 28 , No. 3, page 2290 (1981).

6. Ibid, page 2323.

7. L.R. Evans and R.E. Shafer, Proc. Workshop on Intensity Limitations in Storage Rings, BNL 57236, page 68 (1979).

8. A. Barisy et al., IEEE Trans. on Nucl. Sci. 28 , page 2180 (1981).